Global and Planetary Change 79 (2011) 275–287

Contents lists available at ScienceDirect

Global and Planetary Change

journal homepage: www.elsevier.com/locate/gloplacha

A first evaluation of the spatial gradients in $\delta^{18}O$ recorded by European Holocene speleothems

F. McDermott [a,*], T.C. Atkinson [b], I.J. Fairchild [c], L.M. Baldini [d], D.P. Mattey [e]

[a] UCD School of Geological Sciences, University College Dublin, Belfield, Dublin 4, Ireland
[b] Department of Earth Sciences, Pearson Building, University College London, Gower Street, London WC1E 6BT, UK
[c] School of Geography, Earth and Environmental Sciences, University of Birmingham, Edgbaston, Birmingham B15 2TT, UK
[d] Department of Earth Sciences, University of Durham, Durham, DH1 3LE, UK
[e] Department of Earth Sciences, Royal Holloway, University of London, Egham, Surrey, TW20 0EX, UK

ARTICLE INFO

Article history:
Received 17 July 2010
Accepted 20 January 2011
Available online 5 February 2011

Keywords:
speleothems
oxygen isotopes
palaeoclimate
Holocene
isotope gradients

ABSTRACT

Oxygen isotope data for well dated Holocene speleothems from Europe have been compiled for the first time. The data were analysed at 1 ka time slices through the Holocene by taking averages of 50 year duration. After filtering the data to exclude high altitude, high latitude and sites proximal to the Mediterranean Sea, the data exhibit surprisingly tight linear correlations between speleothem O isotope values and longitude. The slope of the data on $\delta^{18}O$ vs. longitude plots changes systematically from the early to the late Holocene, exhibiting a much steeper zonal gradient in the early Holocene. Changes in the isotope gradient through the course of the Holocene reflect both a gradual increase in $\delta^{18}O$ in speleothems from the western margin of the transect and a simultaneous decrease in speleothem $\delta^{18}O$ on the eastern end of the transect. These changes follow summer insolation trends through most of the Holocene, but show marked deviations from c. 4 ka to the present day. Steeper early Holocene zonal isotope gradients are attributed primarily to a combination of early Holocene warming in the west and intense convective rainfall over the European continent in summer time driven by high early Holocene summer insolation. Although the absolute $\delta^{18}O$ values preserved in speleothems do not precisely reflect the equilibrium values with respect to the waters from which they are precipitated, the tight isotope-longitude correlations indicate that speleothems are reliable recorders of combined rainfall O isotope signals and air temperature.

© 2011 Elsevier B.V. All rights reserved.

1. Introduction and rationale for the study

Speleothems are increasingly regarded as valuable archives of past climatic conditions. Unlike most other continental palaeoclimate archives, they can be dated precisely by U-series methods, facilitating comparisons and correlations with independent records such as ice cores. However, as discussed in recent reviews (McDermott, 2004; White, 2004; McDermott et al., 2006; Fairchild et al., 2006; in press; Lachniet, 2009; Fairchild and Treble, 2009), the response to climatic conditions of some commonly measured parameters in speleothems (e.g. $\delta^{18}O$) can be influenced by regional and site-specific factors. It is now well understood that the links between the $\delta^{18}O$ of speleothem calcite ($\delta^{18}O_{spel}$) and specific climate variables such as mean annual air temperature (MAAT), precipitation amount and humidity can vary in space and time, and that the correct interpretation of $\delta^{18}O_{spel}$ typically requires additional data and information.

In some climate zones, the interpretation of $\delta^{18}O_{spel}$ in terms of climatic variables is relatively straightforward because the climate related signals are strong. Thus, in regions influenced by strong monsoonal activity, high amplitude changes in $\delta^{18}O_{spel}$ predominantly reflect insolation-driven changes in monsoon strength (e.g. Fleitmann et al., 2003, 2004; Wang et al., 2001; Cheng et al., 2009) and/or meridional shifts in the position of the ITCZ (Cruz et al., 2006). Similarly, in low- to mid-latitude caves, where speleothem deposition can continue during glacials, the first-order glacial/interglacial transitions can be discerned unambiguously in the $\delta^{18}O_{spel}$ data, facilitating climatic interpretations (e.g. Bar-Matthews et al., 2000; Genty et al., 2003; 2006; Wainer et al., 2009; Williams et al., 2005). It is also increasingly clear that the relatively large amplitude changes in $\delta^{18}O_{spel}$ that often accompany major glacial/interglacial transitions, interstadial events and changes in monsoon strength are too large to ascribe solely to changes in mean annual air temperature (MAAT), and additionally must reflect shifts in precipitation amount or the $\delta^{18}O$ of precipitation as a result of climate-driven changes in vapour sources and moisture transport pathways.

By contrast with the regions mentioned above, Holocene speleothems from the mid- to high-latitude temperate zones of the northern hemisphere (e.g. N.W. Europe) typically exhibit relatively small ranges in $\delta^{18}O_{spel}$, reflecting weaker climate signals and the well-documented competing influences on $\delta^{18}O_{spel}$ (e.g. McDermott,

* Corresponding author.
E-mail address: frank.mcdermott@ucd.ie (F. McDermott).

0921-8181/$ – see front matter © 2011 Elsevier B.V. All rights reserved.
doi:10.1016/j.gloplacha.2011.01.005

2004; Fairchild et al., 2006). Thus, $\delta^{18}O_{spel}$ in mid-latitude European Holocene speleothems typically varies by approximately ±1‰ around the long-term mean, in datasets with a decadal-scale resolution. A more robust interpretative framework is required therefore for these regions, and in particular a methodology is required to distinguish the relatively weak regional scale climate signals from local site-specific 'noise' (e.g. changes in speleothem $\delta^{18}O$ that might arise from local hydrological routing effects, evaporation of water at or near the surface and/or non-equilibrium depositional effects (Baker and Bradley, 2009).

With few exceptions (e.g. Lachniet et al., 2007) studies of $\delta^{18}O$ variability in speleothems have focused on reconstructing time-series records for individual stalagmites, but relatively little attention has been paid to the $\delta^{18}O_{spel}$ variations in coeval stalagmites from the same region. This is somewhat surprising given (1) the tight chronological control on most $\delta^{18}O_{spel}$ time-series datasets that permits such comparisons, and (2) the need for better inter-site replication to distinguish regional-scale climate signals from local site-specific noise. In this study, the available O isotope time-series records for European Holocene speleothems have been compiled, better to understand the spatial patterns and continent-scale gradients in $\delta^{18}O_{spel}$ through time since the early Holocene. Because the conclusions drawn are based on several independently studied speleothems, this approach has the potential to provide robust insights, and to test interpretations that were based solely on single time-series records.

It is well known that $\delta^{18}O$ in meteoric water ($\delta^{18}O_{mw}$) varies spatially as a function of latitude, altitude, continentality, mean annual temperature and rainfall amount on the scale of the European continent in the present day (e.g. Rozanski et al., 1982; Rozanski et al., 1993; Bowen and Wilkinson, 2002). Ignoring local orographic effects, such variations in $\delta^{18}O_{mw}$ are characterised by relatively smooth meridional and zonal gradients, reflecting gradual and progressive rainout from air masses with decreasing MAATs, and increasing continentality respectively. Crucially, as more speleothem O isotope records are published, the spatial density of the European Holocene speleothem $\delta^{18}O$ dataset is now beginning to rival that of the Global Network of Isotopes in Precipitation (GNIP) network within mainland Europe and the surrounding circum-Mediterranean region.

$\delta^{18}O_{spel}$ is influenced by both the $\delta^{18}O$ value of the cave drip water from which it is deposited ($\delta^{18}O_{drip}$) and the cave air temperature. In many, but not all caves, cave air temperatures closely approximate the MAATs of the region above the cave (Wigley and Brown, 1976). Exceptions include cave systems that exhibit cold-trap behaviour and/or strong seasonal ventilation effects (e.g. Spötl et al., 2005). Several drip-water monitoring studies have shown that the aquifer residence time of cave drip waters that are supersaturated with respect to calcite, and are therefore capable of precipitating speleothems, usually exceeds one year (Baldini, 2004; Fuller et al., 2008). As a result, $\delta^{18}O_{drip}$ variations in drips that deposit speleothems are normally strongly attenuated with respect to the seasonal range in $\delta^{18}O_{mw}$ (Yonge et al., 1985; Caballero et al., 1996) and tend to preserve annual average rather than seasonal $\delta^{18}O_{mw}$ signals.

Additionally, it has been shown that speleothem calcites are seldom deposited precisely at the expected equilibrium value ($\delta^{18}O_{equil}$) with respect to their drip waters (Mickler et al., 2004; McDermott et al., 2006), and that kinetic effects are important (Coplen, 2007; Dietzel et al., 2009). In general, $\delta^{18}O_{spel}$ tends to be offset by 1.0±0.5‰ compared with that predicted by both the Kim and O'Neil (1997) and Coplen (2007) equations, reflecting a degree of disequilibrium (McDermott et al., 2006). Here we refer to this disequilibrium as Δ_{dis}, where Δ_{dis} is defined as the difference between the observed and calculated equilibrium speleothem $\delta^{18}O$ value ($\delta^{18}O_{spel} - \delta^{18}O_{equilibrium}$). The magnitude of Δ_{dis} is discussed in more detail below.

With some assumptions about the magnitude of Δ_{dis}, and the likely (relatively small) low-frequency changes in MAAT during the Holocene in Europe (e.g. Mayewski et al., 2004; Wanner et al., 2008), interpolations based on the published Holocene $\delta^{18}O_{spel}$ dataset can be used to infer past $\delta^{18}O_{mw}$ gradients. These isotope gradients could in turn may be used to: (1) recognise anomalous $\delta^{18}O_{spel}$ values that could reflect local site-specific effects and/or systematic seasonal biases, (2) provide comparisons with past $\delta^{18}O_{mw}$ values reconstructed from speleothem fluid inclusion studies and (3) provide 'baseline' $\delta^{18}O_{spel}$ values against which higher frequency (decadal to centennial scale) $\delta^{18}O_{spel}$ variability can be compared. Inferences about gradients in Holocene speleothem $\delta^{18}O$ can also be checked against those inferred from other secondary carbonates (e.g. tufa deposits and lake marls) to improve the reliability of speleothem-based palaeoclimate interpretations, and to isolate local departures from the expected smooth regional scale gradients (e.g. due to evaporative and/or hydrological effects). The primary aim of this study is to provide a preliminary assessment of the spatial gradients in $\delta^{18}O_{spel}$ within Europe through the Holocene, and to identify temporal changes in these gradients that could reflect changes in climatic conditions and/or vapour source changes. In future, the inferred isotope gradients can also be compared with the output of 'isotope enabled' general circulation models (GCMs) to test and validate their physics and assumptions.

Our approach necessarily requires temporal averaging of the $\delta^{18}O_{spel}$ time-series data and a consequent loss of temporal resolution, but it is likely to provide a more robust view than that based on single sites considered in isolation, especially if key variables (e.g. temporal changes in MAAT) can be estimated independently (e.g. by the European pollen database). A secondary aim of this study is to distinguish between sites in Europe that are influenced primarily by either Atlantic or Mediterranean moisture sources, and to assess how the relative importance of these sources may have changed during the course of the Holocene.

2. The dataset and methodology

The published and available unpublished oxygen isotope data for European (sensu-lato) Holocene speleothems have been compiled (Table 1). Only those speleothems for which reliable thermal ionisation mass-spectrometric (TIMS) or multi-collector inductively coupled plasma mass-spectrometry (MC-ICP-MS) U-series chronologies available were included in the compilation; speleothems that were dated exclusively by alpha-spectrometry or by ^{14}C were excluded, because of their unacceptably large age uncertainties. Only calcite speleothems were included. Aragonite speleothems were omitted to avoid possible biases in $\delta^{18}O$ due to mineralogical effects on the stable isotope fractionation factors (Grossman and Ku, 1986). This resulted in a dataset of 53 (discontinuous) Holocene speleothem records from 37 cave sites (Table 1), that extend from southern Spain to northern Norway, and from S.W. Ireland to Israel (Fig. 1). The emphasis in this paper is on delineating the first-order low frequency spatial gradients in European speleothem $\delta^{18}O$ through time, and for this reason our focus is on short 'snapshots' (50 year averages of $\delta^{18}O_{spel}$) taken at 1000 year intervals through the Holocene (Table 1). Whenever possible, the averages were calculated from available time-series digital data files, but in some cases where it was not possible to obtain the original data files, these values were estimated visually from published time-series graphs. Table 1 lists the latitude, longitude and altitude of each cave site as well as the calculated mean $\delta^{18}O$ for each 50 year snapshot at 1000 year intervals from 12 ka to the present-day. Table S1 provides a summary of the data sources for each site.

3. Results from the compiled datasets

In Fig. 1, contours of present-day $\delta^{18}O_{spel}$ values reveal several important spatial trends. The major trend is one of gradually decreasing $\delta^{18}O_{spel}$ in an east–northeasterly direction from the

Table 1
Compilation of speleothem $\delta^{18}O$ for European Holocene stalagmites from the literature and unpublished sources. Data sources are given in Table S1. Latitude and longitude values are in degrees. Elevation values (Elev.) are in metres above sea level. Present-day speleothem $\delta^{18}O$ values are given as 0 ka. The column 'Drip' reports the mean $\delta^{18}O$ (V-SMOW) value for present-day drip water at each site. Other data are 50 year average 'snapshot' values at 1 ka intervals (e.g. the data for 1 ka is the mean $\delta^{18}O$ value for time-series speleothem carbonate that was deposited between 1025 and 975 years before present). Superscript numbers in 'speleothem' column are linked to data sources given in Table S1.

Country	Cave	Speleothem	Lat (N)	Long (E)	Elev.	T (°C)	Drip	0 ka	1 ka	2 ka	3 ka	4 ka	5 ka	6 ka	7 ka	8 ka	9 ka	10 ka	11 ka	12 ka
Italy	Carburangeli	CR1[1]	38.15	13.20	22	19.4	−6.00	−6.70	−5.50					−5.50	−6.20	−5.25				
Spain	Pindal	Cand/Maria[2]	43.23	−4.30	24	13.0									−4.75	−4.60	−4.80	−4.30	−4.25	−4.20
Ireland	Crag	CC3[3]	52.23	−9.44	60	10.4	−5.60	−3.80	−3.20	−3.20	−3.20	−4.20	−3.60	−2.90	−3.60	−2.80	−3.00	−3.00		
Ireland	Crag	Bilbo[4]	52.23	−9.44	60	10.4	−5.60	−3.54												
France	Clamouse	CL26[5]	43.7	3.60	75	14.5	−6.20	−4.95	−4.89	−4.79	−4.48	−4.64	−4.76	−4.76	−4.78	−5.00	−4.98	−5.02	−4.94	
France	Clamouse	CL27[6]	43.7	3.60	75	14.5	−6.20	−5.50	−5.70	−5.25										
Spain	Garma	Gar-01[7]	43.43	−3.66	75	12.1	−6.10	−3.99	−4.01	−3.97	−3.90	−4.53	−4.74	−4.39	−4.27	−4.88	−3.81	−3.90	−4.34	−3.99
Spain	Garma	Gar-02[8]	43.43	−3.66	75	13.0	−5.40	−4.48	−4.47											
Lebanon	Jeita	JeG-Stm-1[9]	32.93	35.64	100	22.0			−4.80	−4.60	−5.00	−5.00	−4.70	−5.00	−5.65	−5.60	−5.70	−5.50	−4.80	−4.50
England	Brown's Folly	Boss, BFM9[10]	51.38	2.30	180	10.0		−4.50												
France	Villars	Vil-11[11]	45.5	0.50	175	12.2	−6.33							−4.50	−4.30	−4.75	−4.30	−4.20	−4.10	−4.25
Belgium	Pere Noel	PN95[12]	50.13	5.16	180	9.6	−5.50				−4.65	−5.40	−5.08	−5.07	−5.76	−5.27	−5.27	−5.12	−6.05	−5.70
Belgium	Han-sur-Lesse	Prosperine[13]	50.13	5.16	180	9.0	−7.50	−5.50	−6.00	−6.20										
Belgium	Han-sur-Lesse	Han-stm5b[14]	50.13	5.16	180	8.9	−7.50	−5.55												
Germany	B-7	B7-1[15]	49	7.00	185	9.4	−8.37							−5.40	−5.50	−5.75	−5.30			
Germany	B-7	B7-5[16]	49	7.00	185	9.4	−8.37	−5.70	−5.80	−5.85	−6.05	−6.00	−6.05	−5.80	−5.75	−6.00	−6.00			
Germany	B-7	B7-7[17]	49	7.00	185	9.4	−8.37		−5.50	−5.90	−6.00	−6.10		−5.30	−5.10	−5.20	−5.20			
France	Chauvet	Chau-stm6[18]	44.23	4.26	240	13.2	−6.80													−5.00
Israel	Nahal Qanah	NQ382[19]	32.15	35.1	260	19.0	−5.00	−5.30	−5.30	−5.10	−5.80	−5.40	−6.25	−5.90						
Norway	Rana	SG93[20]	67.54	13.0	280	2.8	−10.0		−7.57	−7.50	−7.63	−7.80	−7.65	−7.45	−7.38	−7.40				
Norway	Rana	SG95[21]	67.54	13.0	280	2.8	−10.0	−7.33	−7.25	−7.20	−7.35	−7.33								
Norway	Rana	SG92-4[22]	67.54	13.0	280	2.8	−10.0						−7.53	−7.75	−7.10					
Italy	Buca de'Renella	RL4[23]	45.0	10.0	300	12.0			−4.25	−3.75	−3.60	−3.30	−3.60	−3.85	−3.75					
England	Lancaster Hole	LH70[24]	54.1	−2.10	294	10.0						−4.60	−4.36	−4.59	−4.62	−3.72	−4.13	−3.94	−3.64	−3.82
Scotland	Uamh an Tartair	SU[25]	58.15	−4.98	220	7.2	−7.1	−5.20	−4.20	−5.00	−4.82									
Romania	Poleva cave	PP10[26]	44.70	21.73	390	10.75					−7.75	−7.63	−7.75	−8.13	−8.30	−8.00	−8.75	−8.88	−8.25	−9.75
Romania	Poleva cave	PP9[27]	44.70	21.73	390	10.75		−8.62	−8.30	−7.88	−7.75	−7.63	−7.75	−7.80	−8.30	−8.00	−8.70	−8.88		
Gibraltar	New St Michael's	Gib04a[28]	36.15	−5.35	400	18.30	−5.00	−5.00												
Israel	Soreq	Sample 2-6[29]	31.75	35.02	400	20.30	−5.00	−5.17	−6.70	−7.30										
Israel	Soreq	Sample 2-N[30]	31.75	35.02	400	20.30	−5.00		−5.40	−5.30	−5.60	−5.40		−5.60	−6.00	−6.20	−6.00	−6.00	−5.50	−4.30
Turkey	Sofular	So-1[31]	41.42	31.93	400	12.00		−8.29	−8.18	−8.01	−8.04	−8.29	−8.32	−7.97	−8.34	−8.54	−9.38	−10.42	−11.21	−11.98
Italy	Savi	SV1[32]	45.61	13.88	441	12.30	−7.28	−6.10	−6.70	−6.32	−6.62	−6.58	−6.48	−6.74	−6.53	−6.70	−6.85	−6.81	−6.53	−6.15
Romania	(Ursilor Cave	PU2[33]	46.32	22.25	482	9.81	−10.3	−7.80												
Slovenia	Postojna	Pos-stm4[34]	45.77	14.22	529	8.00	−9.20	−6.70												
Serbia	Ceremosjna cave	CC-1[35]	45.00	21.0	530	11.6		−6.60	−7.25	−7.20										
Sweden	Korallgrotten	K1[36]	64.88	14.15	570	1.40		−8.55						−9.20	−9.10	−9.25	−9.30			
Spain	Refugio	REF-01[37]	36.50	−4.67	625	17.5		−3.60	−4.40	−4.40										
Spain	Refugio	REF-02[38]	36.50	−4.67	625	17.5	−5.0					−4.80	−5.00							
Spain	Refugio	REF-03[39]	36.50	−4.67	625	17.5					−4.42			−4.58						
Spain	Refugio	REF-04[40]	36.50	−4.67	625	17.5			−4.94	−4.57	−4.46	−5.26								
Sweden	Labyrintgrotten	L4[41]	66.05	14.67	730	−0.5										−9.40	−9.05			
Spain	Kaite cave	LV-5[42]	43.03	−3.65	860	10.4			−6.20	−6.38	−6.10	−6.80			−6.00	−6.50				
Tunisia	La Mine Cave	Min-stm1[43]	36.03	9.68	975	19.5	−6.20							−6.80	−7.00	−7.25	−7.10	−6.75	−6.80	−6.20
Italy	Ernesto	ER76[44]	45.96	11.65	1165	6.7	−9.60	−7.80			−7.80	−7.60	−7.80	−7.60	−7.90	−7.50				
Italy	Ernesto	ER77[45]	45.96	11.65	1165	6.7	−9.60	−7.40												
Italy	Corchia	CC26[46]	44.00	10.22	1300	7.5	−7.40		−4.34	−4.27	−4.30	−4.36	−4.48	−4.49	−4.57	−4.94	−4.46	−4.50	−4.40	−4.15
Germany	Hölloch Cave	Stal-Hoel-1[47]	47.00	10.00	1440	3.5	−11.8	−7.97	−8.07	−8.22	−8.27	−8.57	−8.00	−8.27	−8.47	−8.47	−8.47	−8.90	−8.87	−10.87
Austria	Spannagel	SPA12[48]	47.09	11.67	2347	1.9	−11.3	−7.49	−7.47	−7.40										
Austria	Spannagel	COMNISPA[49]	47.09	11.67	2500	1.9	−11.3	−7.90	−7.90	−7.60	−7.70	−7.50	−7.80	−7.50	−8.00	−7.75	−8.25			
Austria	Katerloch	K1[50]	47.08	15.55	900	8.8	−8.80									−6.41	−6.67	−7.09		
Austria	Katerloch	K3[51]	47.08	15.55	900	8.8	−8.80									−6.29	−5.99	−6.71		
Germany	Attahohle	AH-1[52]	50.80	7.44	308	9.4	−8.92			−6.25	−6.20	−6.20	−6.20							
Norway	Okshala	FM3[53]	67.00	15.00	200	3.2		−7.06									−6.41	−6.67	−7.09	

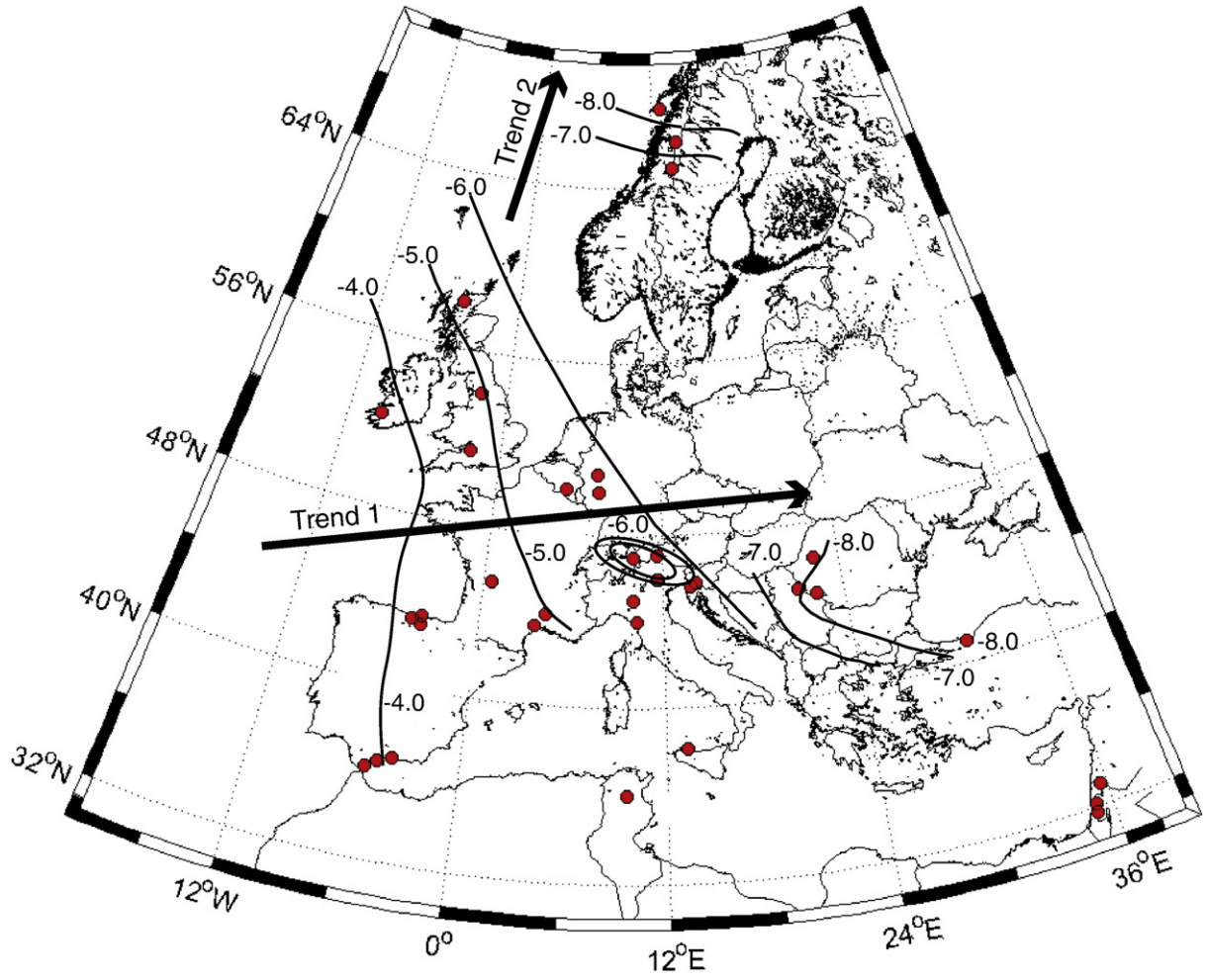

Fig. 1. Map showing locations of cave sites from which speleothem records covering part or all of the Holocene were compiled. Contours are based on $\delta^{18}O_{spel}$ values for recently deposited (zero-age calcite) at these cave sites. Trends 1 and 2 are described in the text. The altitudinal effect on $\delta^{18}O_{spel}$ in the region surrounding the Alps is clearly visible.

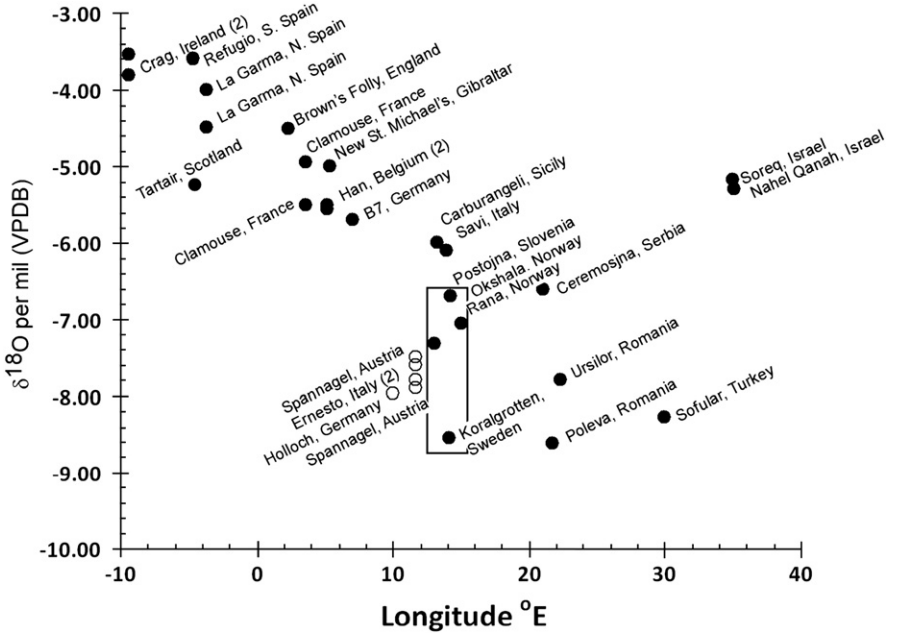

Fig. 2. Present-day $\delta^{18}O_{spel}$ values against the longitude of each cave site. Open data symbols denote high elevation Alpine sites. The data points enclosed by the rectangular box are from the high latitude Scandinavian sites. Data sources are listed in Table S1 (Supplementary material).

oceanic western margin (S.W. Ireland), into continental Europe, south of c.56°N (Trend 1, Fig. 1). North of 56°N, $\delta^{18}O_{spel}$ values also decrease progressively northwards from Scotland through Scandinavia, reflecting a latitudinal effect (Trend 2, Fig. 1). Whereas previous spatial analyses of $\delta^{18}O_{mw}$ on a global scale have emphasised the meridional trends that reflect gradual rainout from northerly advected atmospheric moisture (e.g. Rozanski et al., 1993; Bowen and Wilkinson, 2002), the European speleothem data examined here exhibit much more striking zonal trends, probably reflecting the spatial distribution of the data in relation to the predominant Atlantic moisture source and the strength of the continentality effect in this latitudinal band.

$\delta^{18}O_{spel}$ values in the circum-Mediterranean region are elevated relative to other sites at similar longitudes and this effect is particularly evident in the eastern Mediterranean (Israeli and Lebanese sites). Additionally, Alpine sites in S. Germany, Austria and N. Italy exhibit markedly lower $\delta^{18}O_{spel}$ values (<−6 ‰) compared with other European sites at similar longitudes (Fig. 1), reflecting a clear altitudinal effect. On the basis of the spatial patterns in Fig. 1 we therefore distinguish four important influences on the pattern of $\delta^{18}O_{spel}$ variability in the present-day, namely trends 1 and 2 delineated in Fig. 1, an altitudinal effect (lower $\delta^{18}O_{spel}$) and a Mediterranean Sea vapour source influence (higher $\delta^{18}O_{spel}$).

Fig. 2 shows $\delta^{18}O$ values for the tops of actively growing speleothems (recently deposited calcite), plotted against the longitude of each cave sites. High $\delta^{18}O$ values occur at or close of the North Atlantic margin (e.g. Crag Cave, Ireland, Refugio and La Garma caves in Spain), and values decrease systematically across Europe. At several sites, two or more present-day calcite $\delta^{18}O$ values are available (e.g. Crag cave, Cuevo de la Garma, Grotte de Clamouse, Grotta di Ernesto, Spannagel cave, and Soreq cave). In general, the values are in agreement with each other to within approximately 0.8‰, presumably reflecting relatively small intra-site differences in drip-water $\delta^{18}O$ (e.g. Baker and Bradley, 2009), air temperature and/or isotope disequilibrium effects (Δ_{dis}). Such sub-permil differences in $\delta^{18}O_{spel}$ are relatively unimportant in the context of the large (c. 7‰) first-order longitudinal trends in speleothem $\delta^{18}O$ examined here.

The compiled data also show that $\delta^{18}O_{spel}$ values for samples from high-elevation cave sites (e.g. Alpine sites with elevations of >400 m above sea level) are strongly displaced to more negative values, and plot well below the main data trend (open symbols, Fig. 2), consistent with the well known altitude effect on $\delta^{18}O_{mw}$. Similarly, data from the high latitude cave sites (e.g. Rana, Norway and Koralgrotten, Sweden and Uamh an Tartair, N. Scotland, Fig. 1) are displaced to low $\delta^{18}O$ values (rectangular box, and labelled point for Tartair in Fig. 2), reflecting progressive depletion in the $\delta^{18}O$ of northerly advected moisture and precipitation derived therefrom (rainout effect). Modern $\delta^{18}O_{spel}$ values for the Soreq and Nahel Qaneh cave sites (Bar-Matthews et al., 2003; Frumkin et al., 1999) are clearly displaced well above the main European data array in Fig. 2 reflecting their proximity to the Mediterranean Sea.

The magnitude of possible isotope disequilibrium effects (Δ_{dis}) are considered before attempting to establish links between speleothem $\delta^{18}O$ values and the isotopic composition of the waters from which they were deposited. Taking the Kim and O'Neil (1997) equation for example, and making the approximation that $\delta_A - \delta_B \sim 1000 * \ln(\alpha_{A-B})$, it can be shown that $\delta^{18}O_{spel} = \delta^{18}Omw + (18.03 * (1000/T) - 32.17) + \Delta_{dis}$, where T is cave air temperature in Kelvin (Kim and O'Neil equation as revised by Coplen, 2007). In order to assess the magnitude of Δ_{dis}, calcite $\delta^{18}O$ values have been calculated for each of the European cave sites considered here (Table 1) for which drip-water data have been reported (Fig. 3A). Importantly, calculated calcite $\delta^{18}O$ values using the Kim and O'Neil equation are typically lower (more negative) than actual observed values in modern speleothems. A similar calculation using the Coplen (2007) equation yields values that are typically too high (Fig. 3A). Thus, the Kim and O'Neil equation yields temperatures that appear to be too low, whereas Coplen's equation yields values that are too high. Given the current uncertainty about the true value of the relevant isotope fractionation factors, and the likelihood of kinetic effects (Dietzel et al., 2009), we simply note that the natural speleothem calcites plot along trends sub-parallel to the expected equilibrium values, with offsets that depend on the choice of equation. Overall, the calculated calcite $\delta^{18}O$ values are in approximate agreement with the observed values for modern calcite at each site (typically ±1‰ depending on the choice of equation).

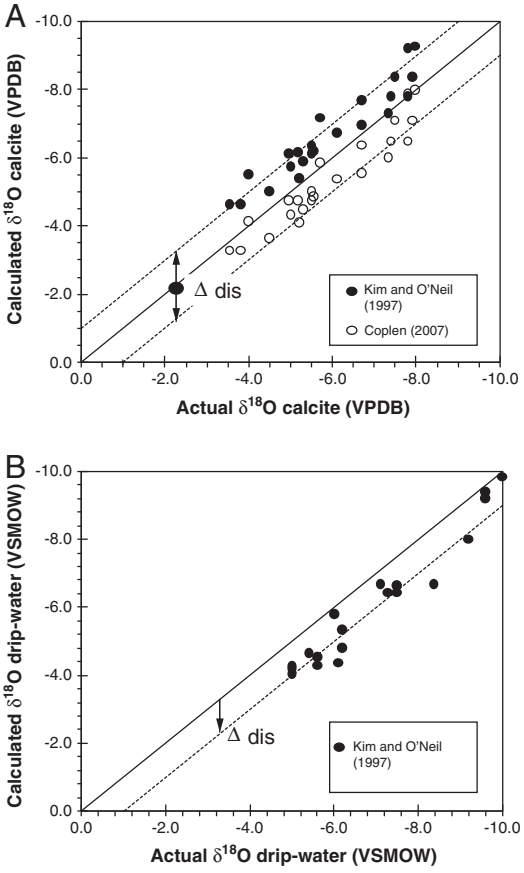

Fig. 3. (A) Calculated $\delta^{18}O$ values (closed symbols, Kim and O'Neil, 1997; open symbols, Coplen, 2007) vs. present-day (zero age) actual $\delta^{18}O_{spel}$ values for cave sites for which both drip-water $\delta^{18}O$ and average air temperatures are known or have been reported in the literature (Table 1). The solid (1:1) line is the locus of points in perfect isotopic equilibrium. The dashed lines are offset by 1‰ above and below (left and right) the 1:1 line. The mean value of Δ_{dis} for all the cave calcites for which all of the required data are available is c. 0.97‰ and an arrow with a length of 1‰ is used in subsequent diagrams to denote Δ_{dis}. (B) Calculated cave drip-water $\delta^{18}O$ values (solid symbols) that would be in equilibrium with the $\delta^{18}O$ values measured in modern (zero age) calcite precipitates in caves, taking account of actual cave temperatures, based on the Kim and O'Neil temperature equation. These values (y-axis), are plotted against actual measured drip-water $\delta^{18}O$ values in the same caves (x-axis). Caves are a sub-set of those in Table 1, selected on the basis that complete drip-water $\delta^{18}O$, modern precipitate $\delta^{18}O$ and cave temperature data were published.

In Fig. 3B, the measured $\delta^{18}O$ values in drip-waters for 23 modern calcite/drip-water pairs for which data have been reported are compared with the Kim and O'Neil (1997) calculated equilibrium values, taking account of the reported cave air temperatures. It is clear that Δ_{dis} is typically about 1‰, with the calculated drip water values displaced to lower $\delta^{18}O$ values compared with the actual measured values (Fig. 3B). Such disequilibrium effects should be considered when calculating equilibrium temperatures from modern drip-water and calcite values, or in calculating the $\delta^{18}O$ values for hypothetical cave drip-waters, assuming a given cave temperature.

While knowledge of Δ_{dis} is important for absolute temperature calculations, the fact that the present-day speleothem calcites define an array that is sub-parallel to the expected 1:1 equilibrium line

(Fig. 3A) suggests that inter-site differences in Δ_{dis} are relatively small (c. 1‰) compared with the overall range (c. 7‰) in $\delta^{18}O_{spel}$ in the European speleothems considered here.

In Fig. 4, calculated $\delta^{18}O$ values for hypothetical cave drip-waters (in equilibrium with the same modern speleothem carbonate samples that were shown in Fig. 2), are plotted as filled circles, based on the assumption of isotopic equilibrium (Kim and O'Neil, 1997), between the drip-waters and the modern cave carbonates and the present-day mean annual air temperature value for each cave. Also shown in Fig. 4 (open circles) are weighted mean $\delta^{18}O$ values for modern rainfall derived from European sites in this longitudinal band from the Global Isotopes in Precipitation (GNIP) database. While the GNIP and cave sites are not, of course, geographically coincident, there is a broad agreement between the weighted mean $\delta^{18}O$ values derived from the GNIP dataset and the calculated $\delta^{18}O_{mw}$ values based on modern calcite precipitates from similar longitudes. Alpine and central European GNIP sites with elevations >400 m above sea level are delineated in the labelled field in Fig. 4, and this field encompasses the alpine cave sites with low $\delta^{18}O_{spel}$ (<−6‰) identified in Figs. 1 and 2. Similarly, the drip-water $\delta^{18}O$ value calculated to be in isotopic equilibrium with the modern Uamh an Tartair speleothem plots below the main data array, reflecting its high latitude. In Fig. 4, it is also evident that calculated $\delta^{18}O$ values for drip-waters in equilibrium with modern speleothem carbonate from Soreq and Nahel Qanah caves are indistinguishable from each other, and plot near the top of the data field for GNIP stations close to the eastern Mediterranean and the Black Sea (Rabba, Bet Dagan, Andana and Kar Kna'an). Inferred drip-water $\delta^{18}O$ values for cave sites that could plausibly be influenced in part by Mediterranean or Black Sea moisture sources (e.g. Sofular cave, Turkey; Ceremosjna cave, Serbia; Grotte di Carburangeli, Sicily; Savi, Italy and Grotte de Clamouse, S.E. France) tend to be relatively high (Fig. 4). The $\delta^{18}O$ values for hypothetical cave drip-waters (filled symbols, Fig. 4) were calculated using the Kim and O'Neil equation and these would be expected to be displaced upwards on the diagram by about 1‰ (to heavier values) as a result of Δ_{dis}, discussed above. This accounts for the observed displacement on Fig. 4 of the values for the hypothetical cave drip-waters towards somewhat heavier values, compared with the GNIP precipitation values at a given longitude. Taking the magnitude of Δ_{dis} into account (c. 1‰) it can be seen that the present-day cave calcites closely reflect the weighted mean $\delta^{18}O$ values for precipitation predicted by the GNIP dataset for any given longitude.

In principle, possible seasonal biases in $\delta^{18}O_{spel}$ as a function of latitude could be evaluated by comparing the $\delta^{18}O_{spel}$ data for modern speleothem carbonates with winter and summer $\delta^{18}O$ data for precipitation at GNIP sites in the same regions, but in practice the differences are too small to evaluate in the light of uncertainties about the appropriate isotope fractionation factors. Seasonal biases could arise from several factors: (1) preferential infiltration of winter rainfall, compensated in some cases by recharge of (^{18}O-enriched) summer rainfall and (2) preferential growth of speleothems in one season, typically winter, from drips that are not well mixed over the annual cycle.

Figs. 5 and 6 show all $\delta^{18}O_{spel}$ data for 1 ka time-slices from 0 ka (present-day) to 12 ka after filtering the data to exclude high latitude sites (Scandinavian sites and Uamh an Tartair, N. Scotland) as well as the high elevation sites distinguished in Fig. 3. In addition to these high latitude and high elevation sites, those within 80 km of the Mediterranean Sea coast (Soreq and Nahel Qanah caves, Israel; Jeita cave, Lebanon; and Corchia cave, Italy) were excluded from the regression calculations in Figs. 5 and 6. The objective of these $\delta^{18}O_{spel}$ vs. longitude diagrams is to delineate the zonal trends and to explore how these may have changed through time. Individual data points represents a c. 50 year averages of $\delta^{18}O_{spel}$, centred on each 1000 year interval. The most important result is that the progressive zonal decreases in $\delta^{18}O_{spel}$, discussed above for the modern speleothem calcites, appear to persist through time, although data are sparser for the early Holocene compared with the late Holocene.

Extrapolation of the regression lines to 10°W for each time slice indicates that in the early Holocene (e.g. at 11 ka), $\delta^{18}O_{spel}$ was higher than in the present day by approximately 0.9‰ in the west, but was simultaneously 1.5‰ lower in the east (e.g. at 30°E). Thus, the

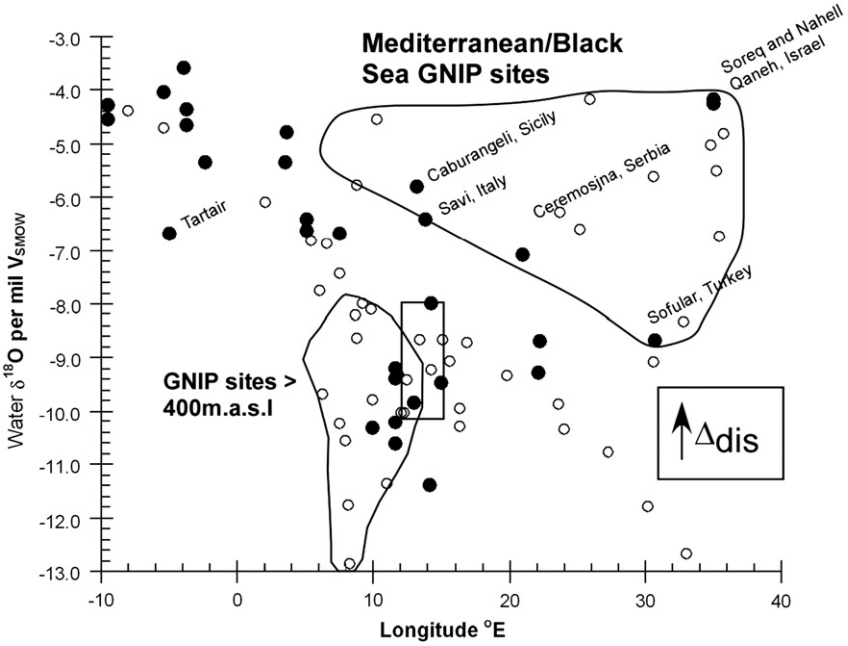

Fig. 4. Calculated $\delta^{18}O$ in hypothetical drip-waters (filled symbols) that would be in isotopic equilibrium with modern carbonate at each of the cave sites shown in Fig. 2. Calculations are based on the equilibrium fractionation factors of Kim and O'Neil (1997), using the specific mean annual temperature of each cave site. Also shown for comparison are $\delta^{18}O$ data for precipitation in Europe (open symbols) as a function of longitude from the GNIP dataset. The arrow labelled Δ_{dis} denotes the sense and magnitude of disequilibrium when the Kim and O'Neil equation is used to calculate the $\delta^{18}O$ values in hypothetical drip-waters (filled symbols).

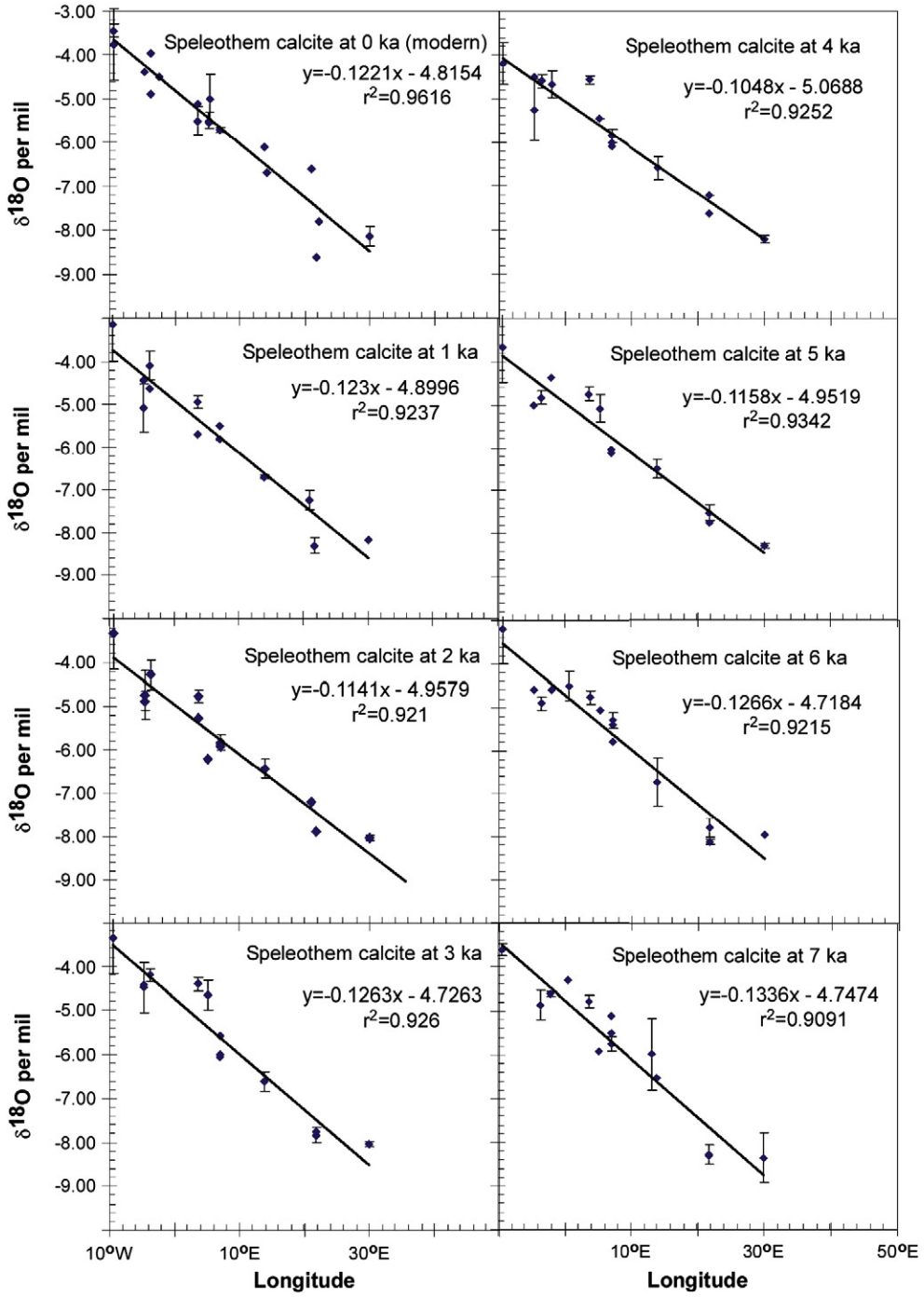

Fig. 5. $\delta^{18}O_{spel}$ vs. longitude for eight 1 ka time-slices in the later Holocene. The data have been filtered for latitude, altitude and proximity to the Mediterranean Sea as explained in the text. Error bars are 1 standard deviation around the plotted mean value for each 50 year time slice. In some cases it was not possible to calculate standard deviations either because the original digital data were unavailable or because too few data points were available for each time slice (e.g. a single measurement of $\delta^{18}O_{spel}$ for modern calcite at some sites).

European $\delta^{18}O_{spel}$ zonal gradient ($d\delta^{18}O_{spel}/dx$) is markedly steeper in the early Holocene (approaching −0.2‰/degree longitude) compared with the mid- to late-Holocene (c. −0.12‰/degree longitude).

Fig. 7 illustrates the extent to which the first-order $\delta^{18}O_{spel}$ trends, calculated on the basis of the 1 ka time-slice $\delta^{18}O_{spel}$ vs. longitude regressions, match the detailed records from a range of sites. Overall, there is good agreement between the predicted first order trends and the individual time-series data trends, reflecting the switch from heavier early Holocene $\delta^{18}O_{spel}$ values in the western end of the transect (e.g. Crag cave and La Garma cave) to lighter early Holocene $\delta^{18}O_{spel}$ values in the east (e.g. Poleva and Sofular). As discussed below, deviations above and below the first-order trends can reflect more regional or even local effects that are not explicable by the superimposed continent-scale air temperature and $\delta^{18}O_{mw}$ fields.

In Fig. 8, the regression line intercepts at 10°W and 30°E as well as the zonal gradients (regression line slopes) for each 1 ka time-slice have been plotted against time. The isotope gradient ($d\delta^{18}O_{spel}/dx$) decreases smoothly between c. 12 ka and 5 ka, but is more variable thereafter (Fig. 8A). Importantly, the decrease in $d\delta^{18}O_{spel}/dx$ through the Holocene reflects *both* elevated $\delta^{18}O_{spel}$ values in the early Holocene on the westerly end of the transect (Fig. 8B) and simultaneously lower values of $\delta^{18}O_{spel}$ on the eastern margin of the

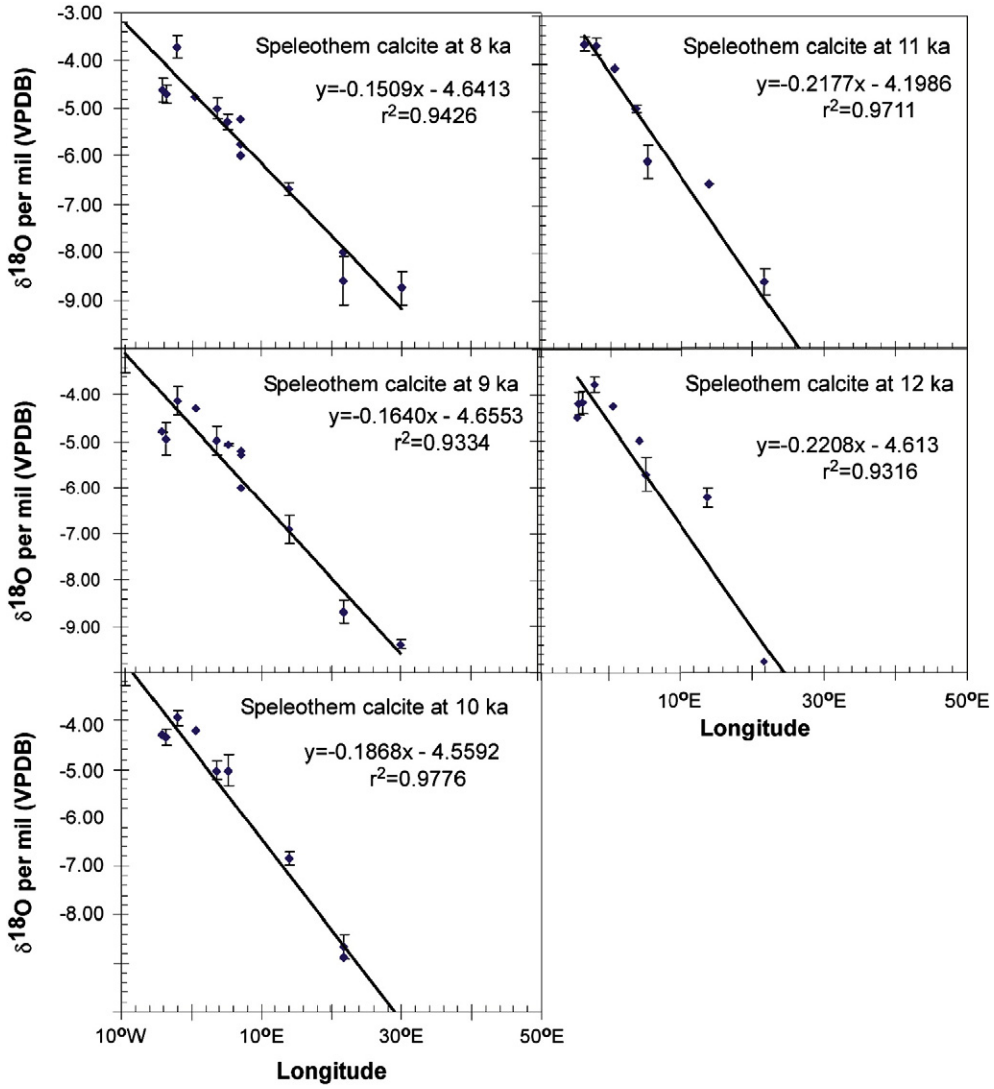

Fig. 6. $\delta^{18}O_{spel}$ vs. longitude for five 1 ka time-slices in the early Holocene. The data have been filtered for latitude, altitude and proximity to the Mediterranean Sea as explained in the text. Error bars are 1 standard deviation around the plotted mean value for each 50 year time slice. In some cases it was not possible to calculate standard deviations either because the original digital data were unavailable or because too few data points were available.

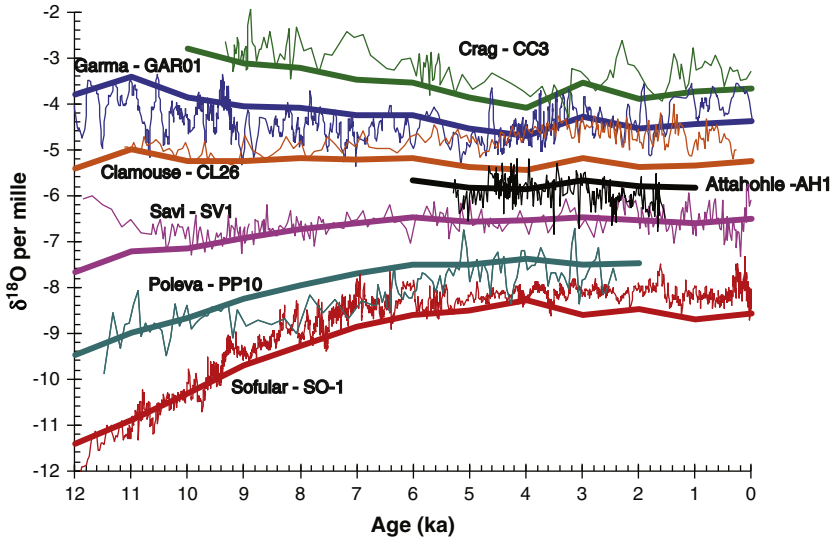

Fig. 7. Comparison of long-term, low frequency time-series trends inferred from the regression equations of Figs. 5 and 6 with the detailed records from several selected Holocene speleothems to illustrate the extent to which the simple longitudinal-based regression can predict the first-order features of the observed time-series data. Typical 1σ variability around the regression-inferred $\delta^{18}O_{spel}$ values (thick curves) is ±0.3‰. Data from sites in western Europe plot close to the top of the diagram and those from eastern Europe plot close to the bottom of the diagram.

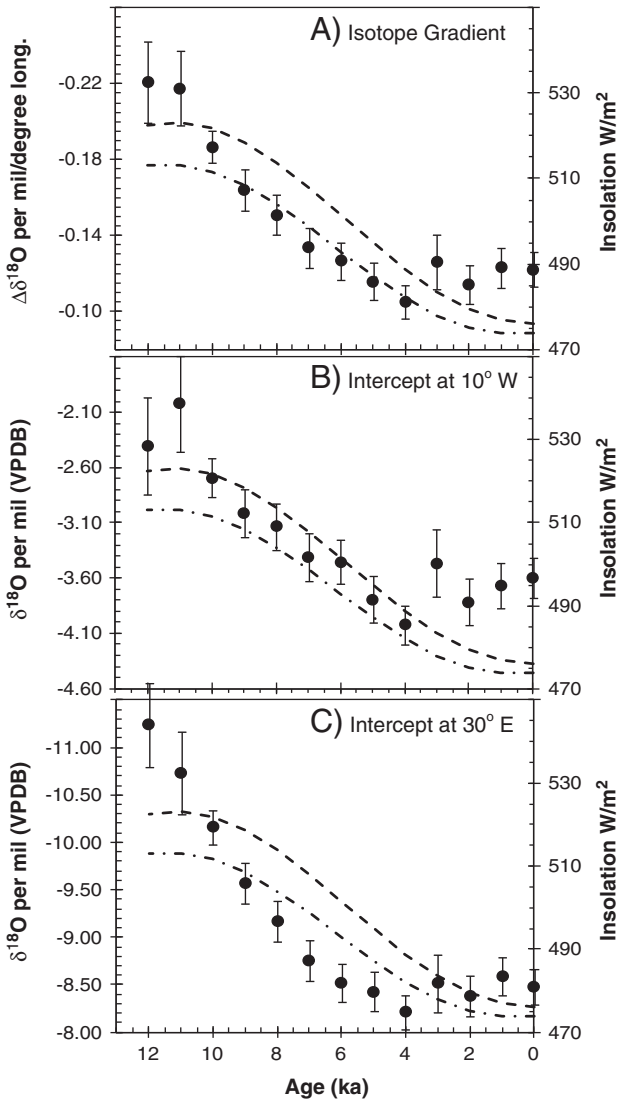

Fig. 8. Plot showing (A) the $\delta^{18}O_{spel}$ gradient calculated by linear regression of data from low elevation, mid-latitude European cave sites, (B) the $\delta^{18}O_{spel}$ intercept at 10°W and (C) the $\delta^{18}O_{spel}$ intercept at 30°E. $\delta^{18}O_{spel}$ values are clearly more depleted in the early Holocene on the eastern margin of the transect compared with the late Holocene. By contrast, $\delta^{18}O_{spel}$ values at the western end of the transect (10°W), calculated from the regression lines are clearly heavier in the early Holocene. Thus, the gradient in $\delta^{18}O_{spel}$ was markedly higher in the early Holocene. Also shown are the June insolation curves for 60°N (dashed lines) and 30°N (dot-dashed lines) after Berger and Loutre, 1991. Error bars are standard errors on the 1 ka time-slice regressions and intercepts.

transect (Fig. 8C). Thus, the value of the intercept at 10°W decreases smoothly through time from approximately -2.1 ± 0.5‰ in the early Holocene to -3.6 ± 0.25‰ after 5 ka (Fig. 8B), while that at 30°W increases from c. −11.25 to -8.5 ± 0.25‰ over the same time interval (Fig. 8C). While data from different cave sites contribute to the calculated regression lines through the Holocene, the easterly sites (Sofular, Turkey and Poleva cave, Romania) are present in all of the regressions, as are the westerly sites of Crag cave (S.W. Ireland) and La Garma cave (N. Spain) indicating that the trends are robust and that the gradients (and calculated intercepts at 10°W and 30°W) are also features of the data for sites through central Europe, west of 25°E.

In summary, the important results of this compilation of speleothem $\delta^{18}O$ data are (1) identification of systematic west-to-east (zonal) decreases in $\delta^{18}O_{spel}$ across Europe that persist throughout the Holocene, (2) a clearly identifiable Mediterranean source effect characterised by relatively high $\delta^{18}O$ for a given value of longitude at some circum-Mediterranean cave sites (e.g. Corchia and Buca della Renella, Italy; Soreq and Nahel Qanah caves in Israel), (3) a clear altitude-related shift to lower $\delta^{18}O_{spel}$ at some Alpine and German sites that have elevations of >800 m (e.g. Spannagel, Austria; Hölloch Cave, S. Germany; and Grotta di Ernesto, N. Italy), (4) low $\delta^{18}O_{spel}$ in the small number of high latitude Scandanavian cave sites (e.g. Rana, Norway; Labyrintgrotten and Korallgrotten, Sweden) in the dataset and (5) systematic temporal changes in the zonal $\delta^{18}O_{spel}$ gradient that appears to reflect *both* a decrease with time in $\delta^{18}O_{spel}$ in the westerly sites (Fig. 8B), and a simultaneous increase in $\delta^{18}O_{spel}$ in the easterly sites from the early to late Holocene.

4. Comparison of speleothem O isotope gradient with other archives

In a compilation of $\delta^{18}O$ and $\delta^{2}H$ data for groundwaters from the U.K., France, Germany, Austria, Hungary, Poland and Romania, Rozanski (1985) demonstrated that the $\delta^{2}H$ of both modern and 'palaeowaters' decrease in an easterly direction across Europe. Inspection of their $\delta^{2}H$-longitude diagram indicates a $\delta^{2}H$-distance slope of approximately 1.05‰ per degree longitude between 10°W and 30°E. Assuming a $\delta^{2}H$–$\delta^{18}O$ relationship similar to that of the modern global meteoric water line, this corresponds to a $\delta^{18}O$ gradient of c. 0.13‰ per degree longitude, similar to that exhibited by the modern and 1 ka $\delta^{18}O_{spel}$ data compiled here (Fig. 5). Darling (2004) also showed that late Pleistocene groundwaters in the interior of the European continent (Austria and Hungary) exhibited much lower (c. 3.5‰) $\delta^{18}O$ values than coeval groundwaters from the western margin of Europe (Portugal). Importantly, this inferred isotope gradient was significantly steeper than that preserved in present-day groundwaters from the same regions, consistent with our observations.

Additional constraints on possible $\delta^{18}O$-distance gradients are provided by stable isotope studies on European tufa deposits. Based on a limited stable isotope dataset for European Holocene tufas, Andrews (2006) demonstrated a progressive shift to lower $\delta^{18}O$ in tufa carbonate ($\delta^{18}O_{tufa}$) in an easterly direction across Europe that he attributed primarily to progressive rainout due to the continentality effect. In this relatively small dataset of seven early Holocene tufas from sites in the U.K., Belgium, Czech Republic, Poland and Belarus, Andrews (2006) identified a c. 5‰ decrease in $\delta^{18}O_{tufa}$ in an easterly direction from the U.K. to Belarus (c. 3°W to 25°E). This implies an isotope gradient of 0.18‰ per degree longitude, very similar to the value of 0.19‰ per degree longitude calculated independently here on the basis of the c. 10 ka old European speleothems (Fig. 6), suggesting that temporal changes in the zonal gradients of $\delta^{18}O_{spel}$ inferred here are robust.

It is noteworthy that the data for the 12 ka time-slice are broadly a continuation of the isotope gradient and intercept trends observed in the early Holocene (Fig. 8), because this time is within the Younger Dryas cold interval. An even steeper zonal gradient in $\delta^{18}O$ was inferred for glacial conditions in Europe (52–24 ka) on the basis of O-isotope data from mammoth tooth enamel samples and a compilation of data for 'palaeogroundwaters' (Arppe and Karhu, 2010).

Data from speleothem fluid inclusions can provide additional constraints and independent checks on spatial gradients in $\delta^{18}O_{spel}$. In a preliminary study of the isotopic composition of fluid inclusions from Holocene stalagmites from GB cave, S.W, England (longitude 2.3°W), Dennis et al. (2001) concluded that the δD values of meteoric water from speleothems deposited since c. 4 ka are broadly similar to those of present-day precipitation. Assuming that constancy in δD is also reflected in $\delta^{18}O_{mw}$, this is consistent with our observation that $\delta^{18}O_{spel}$ values have remained relatively constant since c. 4 ka (e.g. Fig. 8B), with little systematic change in $\delta^{18}O_{spel}$ values during this time interval. Taking into account the longitude of the GB site (2.3°W) and the regression equations for 4 ka to the present-day (Fig. 5),

changes of only ±0.25‰ in $\delta^{18}O_{spel}$ are predicted at this longitude during the past 4 ka.

5. Interpretations and discussion

Trends to lower $\delta^{18}O_{spel}$ across Europe, evident in all of the 1 ka time-slices, are interpreted to reflect progressive distillation and rainout of easterly advected Atlantic-derived water vapour. The persistence of these first-order trends through the Holocene indicates that easterly advection of Atlantic-derived moisture was an enduring feature of atmospheric circulation in this latitudinal band, at least on the millennially spaced 50 year time-slices considered here. Importantly, the relatively good fit of data points to the regression lines indicates that non-equilibrium effects were either relatively small or remained fairly constant spatially and through time. Large variable disequilibrium effects (>1‰) that would significantly disrupt the $\delta^{18}O_{spel}$–longitude correlations are not apparent, suggesting that speleothems can reliably record changing conditions ($\delta^{18}O_{mw}$ and cave air temperature) through time. The temporal changes in longitudinal isotope gradients thus reflect a combination of variations in the superimposed European $\delta^{18}O_{mw}$ and air temperature fields through the Holocene.

Two aspects of the $\delta^{18}O_{spel}$–longitude correlations merit further discussion. First, the cause(s) of the markedly higher early Holocene $\delta^{18}O_{spel}$ values on the western margin (intercept at 10°W) compared with present-day values (Figs. 5 and 6) need to be explained. Second, the steeper $\delta^{18}O_{spel}$–longitudinal gradients in the early Holocene compared with the late Holocene and present-day must be accounted for.

An important factor in explaining the high early Holocene $\delta^{18}O_{spel}$ values on the western margin of Europe is that the $\delta^{18}O$ of the dominant Atlantic vapour source was substantially higher than at present. Much of this difference can be accounted for by the effect of the residual (isotopically depleted) Laurentide and Fennoscandian ice sheets on the isotopic composition of the oceanic vapour source. Post-glacial eustatic sea-level rise in the early Holocene, indicative of the rate of ice sheet decay, can be used to reconstruct temporal changes in the $\delta^{18}O$ of the oceanic source. Using a scaling factor of 0.011‰/m change in sea-level (Fairbanks, 1989), the eustatic sea-level curve (Wanner et al., 2008) indicates that $\delta^{18}O$ in open ocean sources would have been 0.6–0.7‰ higher in the early Holocene (at c. 11 ka) and approximately 0.33‰ heavier at 9 ka (LeGrande and Schmidt, 2009) compared with the present. The extrapolated $\delta^{18}O_{spel}$ values at a longitude of 9.44°W (Crag cave, S.W. Ireland) are somewhat greater than this; c. 0.73‰ higher than present at 11 ka, and c. 0.47‰ higher than present at 9 ka, indicating that much, but perhaps not all of the shift to higher $\delta^{18}O_{spel}$ values in the early Holocene can be accounted for by the ice volume effect. Similarly, in speleothem LH-70s-1 from Lancaster Hole in the U.K. (2.1°W), average $\delta^{18}O_{spel}$ values are approximately 0.8‰ higher at 11 ka and 0.5‰ higher at 9 ka compared with the late Holocene when deposition of this speleothem ceased (at c. 4 ka), again slightly more than can be attributed solely to the ice volume effect. One explanation is that $\delta^{18}O_{mw}$ on the Atlantic margin was higher than that predicted by the ice volume effect alone because of strong early Holocene warming and a positive correlation between $\delta^{18}O_{mw}$ and air temperature (Ahlberg et al., 2001). This inference is consistent with the data from independent biological climate proxies (e.g. pollen, chironomid and coleoptera) that indicate rapid early Holocene onset of warm conditions, especially in summer, on the Atlantic western Europe (e.g. Atkinson et al., 1987; Davis et al., 2003; Gandouin et al., 2007; Ponel et al., 2007).

Evidence for early Holocene warming in the west is also preserved in lake sediment records. In many lake sediment cores from Ireland and Britain the transition from the Younger Dryas to the early Holocene is marked by an abrupt lithological change, marking a rapid transition from predominantly clay-rich detrital inputs in the cold Younger Dryas interval to authigenic carbonate production and organic-rich inputs in the early Holocene (O'Connell et al., 1999; Marshall et al., 2002). Authigenic carbonates from lake sediment cores retrieved from Lough Gur (southwestern Ireland) by Ahlberg et al. (2001) exhibit $\delta^{18}O$ values that are c. 2‰ higher in the early Holocene than the mid-Holocene (c. 6 ka). This is broadly in line with the decrease in $\delta^{18}O_{spel}$ inferred from the spatial correlations for the western end of the speleothem transect presented here (Figs. 5 and 6). Similarly, in a study of late Glacial to Holocene lake carbonates from Lough Inchiquin (western Ireland), Diefendorf et al. (2006) demonstrated that $\delta^{18}O$ values in authigenic calcites increased rapidly at c. 10.5 ka, interpreted to reflect the onset of Boreal warming in western Ireland in the early Holocene.

The first-order $\delta^{18}O_{spel}$–longitude trends across Europe can be explained by a Rayleigh distillation model (Siegenthaler and Matter, 1983) of progressive rainout of easterly advected moisture bearing air masses. A quantitative rainout model constructed here to investigate the effects of several possible variables on the observed spatio-temporal trends considers an oceanic (Atlantic) moisture source region with a $\delta^{18}O$ value close to zero (the source is given higher values in the early Holocene to reflect the presence of continental ice-sheets as discussed above). The temperature at which evaporation of this oceanic source occurred was also allowed to vary, but this has a negligible effect on the $\delta^{18}O$ of the initial vapour. In the model, the vapour was then advected north–easterly and allowed to progressively rainout over the European continental land mass. Standard equations and isotope fractionation factors (Rozanski et al., 1982; Gonfiantini, 1986; Gat, 1996; Lachniet, 2009) were used to model the oxygen isotopic composition of the vapour phase and its subsequent rainout over Europe. In this simple rainout model, R_c is the isotope ratio (e.g. $^{18}O/^{16}O$) of the condensate ($\delta^{18}O_{pption}$), α is the fractionation factor between the condensate and vapour, R_{VO} is the isotope ratio of the initial vapour and F is the mass fraction of vapour remaining. This simple model in which F changes from 0.8 close to the Atlantic coast (e.g. Crag cave site, S.W. Ireland) to 0.5 in east-central Europe can account for the observed c. 6‰ decrease in $\delta^{18}O$ for waters in isotopic equilibrium with present-day speleothem deposits (0 ka $\delta^{18}O_{spel}$ gradient in Fig. 5). This calculation is insensitive to the choice of calcite–water isotope fractionation factors, as these affect only the magnitude of the offset between $\delta^{18}O_{spel}$ and $\delta^{18}O_{mw,}$ but not the rainout slope. As discussed by Siegenthaler and Matter (1983), the dependence of α on temperature is weak, but air temperature exerts a crucial influence on the degree of rainout (1-F) as moisture bearing air masses rain out. Specifically, the temperature difference between the oceanic vapour source and that of the site of condensation (above a cave site), determines the degree of rainout, with higher degrees of rainout (a warmer western margin and a cooler continental interior), giving rise to steeper $\delta^{18}O_{spel}$–longitude gradients. A further result from this simple rainout calculation is that the required change in F (0.8 to 0.5), as a function of longitude across Europe must be relatively steep to account for the slope of the $\delta^{18}O_{pption}$ data inferred to be isotopic equilibrium with the modern $\delta^{18}O_{spel}$ data (Fig. 5). Importantly, the relationship between F and longitude required to model these data is close to the present-day *winter* F vs. longitude relationship for Europe employed in the model of Rozanski et al. (1982), and it contrasts with their shallower summertime rainout slope. One implication is that the $\delta^{18}O_{spel}$ data may predominantly reflect winter precipitation in Europe; summer-time rainout slopes (Rozanski et al., 1982) would produce $\delta^{18}O_{spel}$–longitude trends that are too shallow. It should also be noted that the simple Rayleigh distillation model employed here cannot adequately capture the effects on $\delta^{18}O_{mw}$ of moisture recycling and convective rainfall discussed below.

As discussed, possible explanations for the higher early Holocene $\delta^{18}O_{spel}$ values in the west include (1) an important component from the ice volume effect and (2) higher $\delta^{18}O_{mw}$ caused by differential early Holocene warming, with a steeper mean annual temperature gradient between the Atlantic margin and the continental interior in the early Holocene, compared with the present day. This explanation

assumes a positive correlation between $\delta^{18}O_{mw}$ and condensation temperatures One possibility is that insolation driven changes in the latitude of moisture evaporation from the Atlantic Ocean, led to more proximal sources of Atlantic moisture in the early Holocene. The latter effect would generate higher values of $\delta^{18}O_{mw}$ arriving at the western margin of Europe because moisture-bearing air masses would have undergone less rainout (higher values of F and therefore higher $\delta^{18}O_{mw}$ in the west).

Invoking an insolation-driven change in Atlantic moisture sources (more proximal sources) is speculative, but the isotope gradients and intercepts broadly resemble changes in June insolation between 30 and 60°N (Fig. 8) until c. 4 ka. Long term cooling through the Holocene, in parallel with decline in summer insolation is found in several studies that employ summer-temperature sensitive biological proxies (Naughton et al., 2007; Seppä et al., 2009).

In summary, the steeper gradient in $\delta^{18}O_{spel}$ in the early Holocene likely reflects cooler early Holocene climatic conditions in continental Europe relative to the western Atlantic margin, resulting in lower $\delta^{18}O_{mw}$ in central and eastern Europe as a consequence of both lower moisture condensation temperatures *and* a greater degree of rainout (lower F values) from cooler moisture bearing air masses. Greater contributions from moisture recycled from the surface of the European continent through convective rainfall (e.g. Koster et al., 1993) may also have played a role in generating the steeper early Holocene $\delta^{18}O_{spel}$ gradients. Convective rainfall typically leads to lower $\delta^{18}O$ values in rainfall (Vuille et al., 2003). More intense convective rainfall could result from greater summer heating of the European land surface as a result of higher summer insolation in the early Holocene (Fig. 8), and as discussed above, this could also explain, at least in part, the simultaneously higher $\delta^{18}O_{spel}$ values on the western margin. A similar effect was described recently in Amazonia (van Breukelen et al., 2008). In the latter study, gradually increasing wet-season (January–February) insolation was linked to enhanced convective rainfall and progressively lower $\delta^{18}O$ rainfall (and speleothem) values through the course of the Holocene. In the case of the European dataset, higher summer insolation in the early Holocene could simultaneously drive more proximal derivation of Atlantic moisture and more intense convective rainfall within the European continental landmass, leading to lower $\delta^{18}O$ in rainfall and a steeper isotope gradient eastwards into the continent. This effect would decrease gradually through the course of the Holocene as summer insolation values declined. Colder winter conditions within continental Europe due to lower winter insolation values may also have been a factor in lowering $\delta^{18}O$ in the early Holocene in central Europe.

Although beyond the scope of this study, strong deviations to higher $\delta^{18}O_{spel}$ at a given longitude permit identification of sites at which Mediterranean moisture sources were important on the relatively low-frequency timescales examined here (e.g. Corchia cave, Italy, Israeli and Lebanese cave sites). For example, part of the shift to relatively high $\delta^{18}O_{spel}$ in the late Holocene in speleothem CL26 from Clamouse cave, S. France could reflect greater advection of isotopically heavier Mediterranean-derived moisture. Similarly, in the speleothem from Savi cave (SV-1), the markedly higher $\delta^{18}O_{spel}$ values prior to 10 ka may reflect higher $\delta^{18}O_{mw}$ (Frisia et al., 2005) as a result of greater inputs of Mediterranean-derived moisture. Data for speleothem So-1 from Sofular cave in northwestern Turkey tend to plot on or close to the $\delta^{18}O_{spel}$ vs. longitude regression lines (Figs. 5, 6 and 7), despite the likely input of Black Sea derived moisture (Fleitmann et al., 2009). However, omission of the Sofular data point does not materially affect our conclusions regarding temporal changes in the oxygen isotope gradients through the Holocene. In detail, the isotope gradients are somewhat lower in the early Holocene (slopes of −0.195 and −0.191 for 11 ka and 10 ka respectively without the Sofular data point) compared with −0.218 and −0.221 for 11 ka and 10 ka when the Sofular data are included (Fig. 6).

The isotope gradients and intercepts change markedly between 4 ka and 3 ka (Fig. 8), perhaps implying a shift in atmospheric circulation in the late Holocene. After c. 4 ka, the isotope gradient increases again because $\delta^{18}O_{spel}$ values appear to increase more in the west than in the east (Fig. 8). This effect is seen clearly in the individual records plotted in Fig. 7 as increases in $\delta^{18}O_{spel}$ in the speleothems from Crag cave (CC3), La Garma cave (Gar-01) and Clamouse (CL26).

6. Conclusions

$\delta^{18}O_{spel}$ values for European Holocene speleothems decrease as a function of the distance from Atlantic Ocean (longitude) when the data are filtered to exclude (1) high elevation Alpine sites (>600 m), (2) sites close to (<80 km) the Mediterranean Basin coastline and (3) high latitude sites (>56°N). $\delta^{18}O_{spel}$ values, filtered to exclude the three effects listed above, have been calculated at 1 ka intervals through the Holocene based on c. 50 year averages. These data exhibit define tight linear correlations with longitude, but the $\delta^{18}O_{spel}$ vs. longitude gradient changes with time from steeper gradients in the early Holocene to shallower gradients in the mid to late Holocene. While the ice volume effect undoubtedly played an important role in defining the value of $\delta^{18}O_{mw}$ arriving at the western European margin, it cannot by itself account for steeper isotope gradients in the early Holocene. The steeper early Holocene gradient reflects higher $\delta^{18}O_{spel}$ values on the western end of the transect, and simultaneously lower $\delta^{18}O_{spel}$ values in the east. Lower early Holocene $\delta^{18}O_{spel}$ values in the east (central Europe) and associated steeper zonal isotope gradients are attributed to a combination of differential early Holocene warming from west to east, and more intense insolation-driven summer convective rainfall over the continental landmass. This effect decreased during the course of the Holocene as summer insolation declined. After c. 4 ka, the pattern of gradual changes in the O isotope gradient and intercepts in the west and east was interrupted, possibly reflecting a regional-scale reorganisation of atmospheric circulation.

Overall, the data indicate that westerly-derived (Atlantic) moisture sources persisted throughout Holocene, with no major long-term (>50 year) changes in the atmospheric circulation pattern with the latitudinal band considered here. Importantly, the preservation of tight linear correlations between $\delta^{18}O_{spel}$ and longitude indicates that speleothem calcite $\delta^{18}O$ values were not unduly affected by site-specific or variable disequilibrium effects, at least on the multi-decadal timescales considered here (50 year averages).

Finally, we note that because the direction of the transect studied here, constrained by the geographical distribution of European cave sites, is not parallel to the steepest ENE-gradient observed in present-day European precipitation, the O isotope gradients in an ENE direction across Europe may have been somewhat steeper at any given time in the past than implied by the sites considered here.

Supplementary materials related to this article can be found online at doi:10.1016/j.gloplacha.2011.01.005.

Acknowledgements

Several datasets were produced by funding from Science Foundation Ireland (SFI) grants and NERC-funded ASCRIBE project in RAPID programme. The following people generously provided published datasets in digital form for inclusion in this compilation: Mira Bar-Matthews, Silvia Frisia, Andrea Borsato, Dominik Fleitmann, Bogdan Onac, Silvu Constantin, Augusto Mangini and David Domínguez-Villar. The authors also acknowledge constructive and helpful inputs from two anonymous reviewers.

References

Ahlberg, K., Almgren, E., Wright Jr., H.E., Ito, E., 2001. Holocene stable-isotope stratigraphy at Lough Gur, County Limerick, Western Ireland. Holocene 11 (3), 367–372.

Andrews, J.E., 2006. Palaeoclimatic records from stable isotopes in riverine tufas: synthesis and review. Earth Sci. Rev. 75, 85–104.

Arppe, L., Karhu, J.A., 2010. Oxygen isotope values in precipitation and the thermal climate in Europe during the middle to late Weichselian ice age. Quatern. Sci. Rev. 29, 1263–1275.

Atkinson, T.C., Briffa, K.R., Coope, G.R., 1987. Seasonal temperatures in Britain during the past 22,000 years, reconstructed using beetle remains. Nature 325, 587–592.

Baker, A., Bradley, C., 2009. Modern stalagmite $\delta^{18}O$: instrumental calibration and forward modeling. Glob. Planet. Change 71, 201–206.

Baldini, J.U.L. 2004. Geochemical and Hydrological characterisation of stalagmites as palaeoclimate proxies, with emphasis on trace elemental compositions. Unpubl. PhD thesis, University College Dublin. 299 pp.

Bar-Matthews, M., Ayalon, A., Kaufman, A., 2000. Timing and hydrological conditions of Sapropel events in the Eastern Mediterranean, as evident from speleothems, Soreq cave, Israel. Chem. Geol. 169, 145–156.

Bar-Matthews, M., Ayalon, A., Gilmour, M., Matthews, A., Hawkesworth, C.J., 2003. Sea–land oxygen isotopic relationships from planktonic foraminifera and speleothems in the Eastern Mediterranean region and their implications for paleorainfall during interglacial intervals. Geochim. Cosmochim. Acta 67, 3181–3199.

Berger, A., Loutre, M.F., 1991. Insolation values for the climate of the last 10 million of years. Quatern. Sci. Rev. 10, 297–317.

Bowen, G., Wilkinson, B., 2002. Spatial distribution of $\delta^{18}O$ in meteoric precipitation. Geology 30, 315–318.

Caballero, E., Jimenez De Cisneros, C., Reyes, E., 1996. A stable isotope study of cave seepage waters. Appl. Geochem. 11, 583–587.

Cheng, H., Edwards, R.L., Broecker, W.S., Denton, G.H., Kong, X., Wang, Y., Zhang, R., Wang, X., 2009. Ice age terminations. Science 326, 248–252.

Coplen, T.B., 2007. Calibration of the calcite–water oxygen-isotope geothermometer at Devils Hole, Nevada, a natural laboratory. Geocmimica Cosmochim. Acta 71, 3948–3957.

Cruz, J.F.W., Burns, S.J., Karmann, I., Sharp, W.D., Vuille, M., 2006. Reconstruction of regional atmospheric circulation features during the late Pleistocene in subtropical Brazil from oxygen isotope composition of speleothems. Earth Planet. Sci. Lett. 248, 495–507.

Darling, W.G., 2004. Hydrological factors in the interpretation of stable isotopic proxy data present and past: a European perspective. Quatern. Sci. Rev. 23, 743–770.

Davis, B.A.S., Brewer, S., Stevenson, A.C., Guiot, J., Contributors, Data, 2003. The temperature of Europe during the Holocene reconstructed from pollen data. Quatern. Sci. Rev. 22, 1701–1716.

Dennis, P.F., Rowe, P.J., Atkinson, T.C., 2001. The recovery and isotopic measurement of fluid inclusions in speleothems. Geochim. Cosmochim. Acta 65, 871–884.

Diefendorf, A., Patterson, W.P., Mullins, H.T., Tibert, N., Martini, A., 2006. Evidence for high-frequency late Glacial to mid-Holocene (16,800 to 5500 cal yr B.P.) climate variability from oxygen isotope values of Lough Inchiquin, Ireland. Quatern. Res. 65, 78–86.

Dietzel, M., Tang, J., Leis, A. And, Köhler, S.J., 2009. Oxygen isotopic fractionation during inorganic calcite precipitation — effects of temperature, precipitation rate and pH. Chem. Geol. 268, 107–115.

Fairbanks, R.G., 1989. A 17,000-year glacio-eustatic sea level record: influence of glacial melting rates on the Younger Dryas event and deep-ocean circulation. Nature 342, 637–642.

Fairchild, I.J., Treble, P.C., 2009. Trace elements in speleothems as recorders of environmental change. Quatern. Sci. Rev. 28, 449–468.

Fairchild, I.J., Smith, C.L., Baker, A., Filler, L., Spotl, C., Mattey, D., McDermott, F., E.I.M.F., 2006. Modification and preservation of environmental signals in speleothems. Earth Sci. Rev. 75, 105–153.

Fairchild, I.J., Frisia, S., Borsato, A. and Tooth, A.F. 2007. Speleothems. In: Geochemical Sediments and Landscapes (ed. Nash, D.J. and McLaren, S.J.), Blackwells, Oxford (in press). Chapter 7 SPELEOTHEMS, 200–245.

Fleitmann, D., Burns, S.J., Mudelsee, M., Neff, U., Kramers, J., Mangini, A., Matter, A., 2003. Holocene forcing of the Indian Monsoon recorded in a stalagmite from southern Oman. Science 300, 1737–1739.

Fleitmann, D., Burns, S.J., Neff, U., Mudelsee, M., Mangini, A., Matter, A., 2004. Palaeoclimatic interpretation of high-resolution oxygen isotope profiles derived from annually laminated speleothems from Southern Oman. Quat. Sci. Rev. 23, 935–945.

Fleitmann, D., Cheng, H., Badertscher, S., Edwards, R.L., Mudelsee, M., Göktürk, O.M., Fankhauser, A., Pickering, R., Raible, C.C., Matter, A., Kramers, J. And, Tüysüz, O., 2009. Timing and climatic impact of Greenland interstadials recorded in stalagmites from northern Turkey. Geophys. Res. Lett. 36, L19707. doi:10.1029/2009GL040050.

Frisia, S., Borsato, A., Spotl, C., Villa, I.M., Cucchi, F., 2005. Climate variability in the SE Alps of Italy over the past 17,000 years reconstructed from a stalagmite record. Boreas 34, 445–455.

Frumkin, A., Carmi, I., Gopher, A., Ford, D.C., Schwarcz, H.P., Tsuk, T., 1999. A Holocene millennial-scale climatic cycle from a speleothem in Nahal Qanah Cave, Israel. Holocene 9, 677–682.

Fuller, L., Baker, A., Fairchild, I.J., Spötl, C., Marca-Bell, A., Rowe, P., Dennis, P.F., 2008. Isotope hydrology of dripwaters in a Scottish cave and implications for stalagmite palaeoclimate research. Hydrol. Earth Syst. Sci. 12, 1065–1074.

Gandouin, E., Ponel, P., Franquet, E., Vliet-Lanoë, Van, Andrieu-Ponel, V., Keen, D.H., Brulhet, J. And, Brocandel, M., 2007. Chironomid responses (Insect:Diptera) to Younger Dryas and Holocene environmental changes in a river floodplain from northern France (St-Momelin, St-Omer basin). Holocene 17 (3), 331–347.

Gat, J.R., 1996. Oxygen and hydrogen isotopes in the hydrologic cycle. Annu. Rev. Earth Planet. Sci. 24, 225–262.

Genty, D., Blamart, D., Ouahdi, R., Gilmour, M., Baker, A., Jouzel, J., Van-Exter, S., 2003. Precise dating of Dansgaard–Oeschger climatic oscillations in western Europe from stalagmite data. Nature 421, 833–837.

Genty, D., Blamart, D., Ghaleb, B., Plagnes, V., Causse, Ch., Bakalowicz, M., Zouari, K., 2006. Timing and dynamics of the last deglaciation from European and North African $\delta^{13}C$ stalagmite profiles — comparison with Chinese and South Hemisphere stalagmites. Quatern. Sci. Rev. 25, 2118–2142.

Gonfiantini, R., 1986. Environmental isotopes in lake studies. In: Fritz, P., Fontes, J.Ch. (Eds.), Handbook of Environmental Isotope Geochemistry, Vol. 2. The Terrestrial Environment, B. Elsevier, Amsterdam, The Netherlands, pp. 113–168.

Grossman, E.L., Ku, T.-L., 1986. Oxygen and carbon isotope fractionation in biogenic aragonite: temperature effects. Chem. Geol. 59, 59–74.

Kim, S.-T., O'Neil, J.R., 1997. Equilibrium and non equilibrium oxygen isotope effects in synthetic carbonates. Geochim. Cosmochim. Acta 61, 3461–3475.

Koster, R.D., Perry de Valpine, D., Jouzel, J., 1993. Continental water recycline and $H_2^{18}O$ concentrations. Geophys. Res. Lett. 20 (20), 2215–2218.

Lachniet, M.S., 2009. Climatic and environmental controls on speleothem oxygen-isotope values. Quatern. Sci. Rev. 28, 412–432.

Lachniet, M.S., Patterson, W.P., Burns, S.J., Asmerom, Y., Polyak, V.J., 2007. Caribbean and Pacific moisture sources on the Isthmus of Panama revealed from stalagmite and surface water $\delta^{18}O$ gradients. Geophys. Res. Lett. 34. doi:10.1029/2006GL028469.

LeGrande, A.N., Schmidt, G.A., 2009. Sources of Holocene variability of oxygen isotopes in palaeoclimate archives. Clim. Past 5, 441–455.

Marshall, J.D., Jones, R.T., Crowley, S.F., Oldfield, F., Nash, S. And, Bedford, A., 2002. A high resolution Late-Glacial isotopic record from Hawes Water, Northwest England Climatic oscillations: calibration and comparison of palaeotemperature proxies. Palaeogeogr. Palaeoclimatol. Palaeoecol. 185, 25–40.

Mayewski, P.A., Rohling, E.E., Stager, J.C., Karlen, W., Maasch, K.A., Meeker, L.D., Meyerson, E.A., Gasse, F., van Kreveld, S., Holmgren, K., Thorp, J.L., Rosqvist, G., Rack, F., Staubwasser, M., Schneider, R.R., Steig, E.J., 2004. Holocene climate variability. Quatern. Res. 62, 243–255.

McDermott, F., 2004. Palaeo-climate reconstruction from stable isotope variations in speleothems: a review. Quatern. Sci. Rev. 23, 901–918.

McDermott, F., Schwarcz, H.P., Rowe, P.J., 2006. Isotopes in speleothems. In: Leng, M.J. (Ed.), Isotopes in Palaeoenvironmental Research. In Springer, Dordercht, pp. 185–225.

Mickler, P.J., Banner, J.L., Stern, L., Asmerom, Y., Edwards, R.L., Ito, E., 2004. Stable isotope variations in modern tropical speleothems: evaluating equilibrium vs. kinetic isotope effects. Geochim. Cosmochim. Acta 68, 4381–4393.

Naughton, F., Jean-François, B., Sánchez Goñi, M.F., Turon, J.-L., Jouanneau, M., 2007. Long-term and millennial-scale climate variability in northwestern France during the last 8850 years. Holocene 17, 939–953.

O'Connell, M., Huang, C.C., Eicher, U., 1999. Multidisciplinary investigations, including stable-isotope studies, of thinck Late Glacial sediments from Tory Hill, Co. Limerick, western Ireland. Palaeogeogra. Palaeoclimatol. Palaeoecol. 147, 169–208.

Ponel, P., Gandouin, E., Coope, R.G., Andrieu-Ponel, V., Guiter, F., Van Vliet-Lanoe, B., Franquet, E., Brocandel, M., Brulhet, J., 2007. Insect evidence for environmental and climate changes from Younger Dryas to Sub-Boreal in a river floodplain at St-Momelin (St-Omer basin, northern France), Coleoptera and Trichoptera. Palaeogeogr. Palaeoclimatol. Palaeoecol. 245, 483–504.

Rozanski, K., 1985. Deuterium and Oxygen-18 in European groundwaters — links to atmospheric circulation in the past. Chem. Geol. Isot. Geosci. Sect. 52, 349–363.

Rozanski, K., Sonntag, C., Munnich, K.O., 1982. Factors controlling stable isotope composition of European precipitation. Tellus 34, 142–150.

Rozanski, K., Araguás-Araguás, L., Gonfiantini, R., 1993. Isotopic patterns in modern precipitation. In: Swart, P.K., Lohmann, K.C., McKenzie, J., Savin, S. (Eds.), Climate Change in Continental Isotopic Records. Geophysical Monograph, 78. American Geophysical Union, Washington, D.C, pp. 1–36.

Seppä, H., Bjune, A.E., Telford, R.J., Birks, H.J.B., Veski, S., 2009. Last nine-thousand years of temperature variability in Northern Europe. Clim. Past. 5, 523–535.

Siegenthaler, U., Matter, H.A., 1983. Dependence of δ18O and δD in precipitation on climate. Palaeoclimates and Palaeowaters: A Collection of Environmental Isotope Studies. IAEA, Vienna. STI/PUB/621.

Spötl, C., Fairchild, I.J., Tooth, A.F., 2005. Cave air control on dripwater geochemistry, Obir Caves (Austria): implications for speleothem deposition in dynamically ventilated caves. Geochim. Cosmochim. Acta 69, 2451–2468.

Van Breukelen, M.R., Vonhof, H.B., Hellstron, J.C., Wester, W.C.G., Kroon, D., 2008. Fossil dripwater in stalagmites reveals Holocene temperature and rainfall variation in Amazonia. Earth Planet. Sci. Lett. 275, 54–60.

Vuille, M., Bradley, R.S., Werner, M., Healy, R., Keimig, F., 2003. Modeling $\delta^{18}O$ in precipitation over the tropical Americas; 1. Interannual variability and climatic controls. J. Geophys. Res. 8, 4174.

Wainer, K., Genty, D., Blamart, D., Hoffmann, D., Couchoud, 2009. A new stage 3 millennial climatic variability record from a SW France speleothem. Palaeogeogr. Palaeoclimatol. Palaeoecol. 271, 130–139.

Wang, Y.J., Cheng, H., Edwards, R.L., An, Z.S., Wu, J.Y., Shen, C.C., Dorale, J.A., 2001. A high-resolution absolute-dated late Pleistocene monsoon record from Hulu Cave, China. Science 294, 2345–2348.

Wanner, H., Beer, J., Bütikofer, J., Crowley, T.J., Cubasch, U., Flückiger, J., Gosse, H., Grosjean, M., Joos, F., Kaplan, J.O., Küttel, M., Müller, S.A., Prentice, I.C., Solomina, O., Stocker, T.F., Tarasov, P., Wagner, M., Widmann, M., 2008. Mid- to Late Holocene climate change: an overview. Quatern. Sci. Rev. 27, 1791–1828.

White, W.B., 2004. Palaeoclimate records from speleothems in limestone caves. In: Sasowsky, I.D., Mylroie, J. (Eds.), Studies of Cave Sediments. Physical and Chemical Records of Palaeoclimate. Kluwer Academic, New York, pp. 135–175.

Wigley, T.M.L., Brown, M.C., 1976. The physics of caves. In: Ford, D.C., Cullingford, C.H.D. (Eds.), The Science of Speleology. Academic Press, London, pp. 329–358.

Williams, P.W., King, D.N.T., Zhao, J.X., Collerson, K.D., 2005. Late Pleistocene to Holocene composite speleothem O-18 and C-13 chronologies from South Island,

New Zealand — did a global Younger Dryas really exist? Earth Planet. Sci. Lett. 230, 301–317.
Yonge, C., Ford, D.C., Gray, J., Schwarcz, H.P., 1985. Stable isotope studies of cave seepage water. Chem. Geol. 58, 97–105.

Further reading

Baldini, L.M. 2007. An investigation of the controls on the stable isotope signature of meteoric precipitation, cave seepage water and Holocene stalagmites in Europe. Unpubl. PhD thesis, University College Dublin. 338 pp.
Boch, R., Spötl, C., Kramers, J., 2009. High-resolution isotope records of early Holocene rapid climate change from two coeval stalagmites of Katerloch Cave, Austria. Quatern. Sci. Rev. 28, 2527–2538.
Constantin, S., Bojar, A.-V., Lauritzen, S.-E., Lundberg, J., 2007. Holocene and Late Pleistocene climate in the sub-Mediterranean continental environment: a speleothem record from Poleva Cave (Southern Carpathians, Romania). Palaeogeogr. Palaeoclimatol. Palaeoecol. 243, 322–338.
Domínguez-Villar, D., Wang, X., Cheng, H., Martin-Chivelet, J., Edwards, R.L., 2008. A high-resolution late Holocene speleothem record from Kaite Cave, northern Spain: $\delta^{18}O$ variability and possible causes. Quatern. Int. 187, 40–51.
Drysdale, R., Zanchetta, G., Hellstrom, J., Maas, R., Fallick, A., Pickett, M., Cartwright, I., Piccini, L., 2006. Late Holocene drought responsible for the collapse of Old World civilizations is recorded in an Italian cave flowstone. Geology 34 (no. 2), 101–104.
Frisia, S., Borsato, A., Mangini, A., Spotl, C., Madonia, G., Sauro, U., 2006. Holocene climate variability in Sicily from a discontinuous stalagmite record and the Mesolithic to Neolithic transition. Quatern. Res. 66, 388–400.
Horvatincic, N., Bronic, I.K., Obelic, B., 2003. Differences in the ^{14}C age, $\delta^{13}C$ and $\delta^{18}O$ of Holocene tufa and speleothem in the Dinaric Karst. Palaeo3 193, 139–157.
Linge, H., Lauritzen, S.-E., Andersson, C., Hansen, J.K., Skoglund, R.Ø., Sundqvist, H.S., 2009. Stable isotope records for the last 10,000 years from Okshala cave (Fauske, northern Norway), and regional comparisons. Clim. Past Discuss. 5, 1763–1802.
Mangini, A., Spötl, C., Verdes, P., 2005. Reconstruction of temperature in the Central Alps during the past 2000 yr from a $\delta^{18}O$ stalagmite record. Earth Planet. Sci. Lett. 235, 741–751.
Mattey, D., Lowry, D., Duffet, J., Fisher, R., Hodge, E., Frisia, F., 2008. A 53 year seasonally resolved oxygen and carbon isotope record from a modern Gibraltar speleothem: reconstructed drip water and relationship to local precipitation. Earth Planet. Sci. Lett. 269, 80–95.
McDermott, F., Frisia, S., Huang, Y., Longinelli, A., Spiro, B., Heaton, T.H.E., Hawkesworth, C.J., Borsato, A., Keppens, E., Fairchild, I.J., van der Borg, K., Verheyden, S., Selmo, E., 1999. Holocene climate variability in Europe: evidence from $\delta^{18}O$ and textural variations in speleothems. Quatern. Sci. Rev. 18, 1021–1038.
McDermott, F., Mattey, D.P., Hawkesworth, C.J., 2001. Centennial-scale Holocene climate variability revealed by a high-resolution speleothem $\delta^{18}O$ record from S.W. Ireland. Science 294, 1328–1331.
McMillan, E.A. 2006. Tests for palaeoaridity in Holocene stalagmites from SW Europe. Keele University PhD thesis (unpublished).
Niggemann, S., Mangini, A., Richter, D.K., Wurth, G., 2003. A paleoclimate record of the last 17,600 years in stalagmites from the B7 cave, Sauerland. Germany. Quatern. Sci. Rev. 22, 555–567.
Onac, B.P., Constantin, S., Lundberg, J., Lauritzen, S.E., 2002. Isotopic climate record in a Holocene stalagmite from Ursilor Cave (Romania). J. Quatern. Sci. 17, 319–327.
Orland, I.J., Bar-Matthews, M., Kita, N.T., Ayalon, A., Matthews, A. And, Vallet, J.W., 2009. Climate deterioration in the Eastern Mediterranean as revealed by ion microprobe analysis of a speleothem that grew from 2.2 to 0.9 ka in Soreq Cave, Israel. Quatern. Res. 71, 27–35.
Sundqvist, H.S., Holmgren, K., Lauritzen, S.-E., 2007. Stable isotope variations in stalagmites from northwestern Sweden document climate and environmental changes during the early Holocene. Holocene 17 (2), 259–267.
Verheyden, S., Keppens, E., Fairchild, I.J., McDermott, F., Weiss, D., 2000. Mg, Sr and Sr isotope geochemistry of a Belgian Holocene speleothem: implications for palaeoclimate reconstructions. Chem. Geol. 169, 131–144.
Verheyden, S., Nadir, F.H., Cheng, J.J., Edwards, L.R., Swennen, R., 2008. Paleoclimate reconstruction in the Levant region from the geochemistry of a Holocene stalagmite from the Jeita cave, Lebanon. Quatern. Res. 70 (2008), 368–381.
Wurth, G., Niggemann, S., Richter, D.K., Mangini, A., 2004. The Younger Dryas and Holocene climate record of a stalagmite from Hölloch Cave (Bavarian Alps, Germany). J. Quatern. Sci. 19 (3), 291–298.
Zanchetta, G., Drysdale, R.N., Hellstrom, J.C., Fallick, A.E., Isolae, I., Gagan, M.K., Pareschi, M.T., 2007. Enhanced rainfall in the Western Mediterranean during deposition of sapropel S1: stalagmite evidence from Corchia cave (Central Italy). Quaternary Science Reviews 26, 279–286.